# Engineering Ionic and Electronic Conductivity in Polymer Catalytic Electrodes Using the Layer-By-Layer Technique

Tarek R. Farhat and Paula T. Hammond*

*Department of Chemical Engineering, Massachusetts Institute of Technology, Cambridge, Massachusetts 02139*

*Received June 21, 2005. Revised Manuscript Received November 3, 2005*

The platinum loading, electronic and ionic conductivity, tuned porosity, and electrode potential of layer-by-layer (LBL) conducting polymer films for thin film catalytic electrodes are presented. Films of polyaniline (PANi)/poly(acrylic acid) (PAA) or PANi/poly(acrylic acid)-*co*-polyacrylamide (PAA-*co*-PAAm) of 3.0-$\mu$m thickness were pH-tuned to induce porosity as they were assembled. Three different techniques were used to dose the LBL PANi films with platinum. The first method used reductive precipitation of platinum and ruthenium salts adsorbed within LBL films of PANi/PAA-*co*-PAAm. The second method, termed polyelectrolyte colloidal platinum stabilization, was applied to load platinum nanoclusters into LBL films of either PANi/PAA or PANi/poly(styrene sulfonate) films. The third method used a PANi/platinum powder dispersion to load platinum crystals into LBL films of PANi/PAA-*co*-PAAm or poly(2-acrylamido-2-methyl-1-propane sulfonic acid) (PAA-*co*-PAMPS). The first method yielded the best metal loadings with maximum platinum loadings of 0.3 mg cm$^{-2}$, and the resulting Pt-containing PANi/PAA-*co*-PAAm films were further examined for their electrochemical characteristics. The electrode potential and chronopotentiometric current control in the resulting electrodes were examined for the best-performing LBL PANi film assembled in this study. The catalyzed PANi/PAA-*co*-PAAm electrodes exhibited an electrode potential similar to that of pure platinum, a relatively high and stable electrical conductivity of 2.3 S cm$^{-1}$, and an ionic conductivity of up to $10^{-5}$ S cm$^{-1}$.

## Introduction

The process of loading catalysts into conductive substrates plays a significant role in the electrochemical, power, and catalysis industries.[1,2] It is a common practice to load noble metals such as platinum, palladium, and ruthenium into a graphite−polymer slurry in the process of graphite electrode manufacturing.[1,3,4] Researchers seeking an organic material as an alternative to graphite can use conducting polymers.[5−7] Thin films of conducting polymers can be obtained from surface polymerization of monomers,[8−10] electrochemical deposition,[11] spin coating,[12−14] and the layer-by-layer (LBL) technique.[15−22] LBL is a method that enables the nanoscale integration of two polymer systems to assemble a thin film with conducting or insulating properties.[23−25] The advantages gained by using the alternating adsorption of a conducting polymer with a second polymer include tuning of the nanocomposite structure to exhibit (i) better surface uniformity and mechanical stability,[15,26] (ii) capability of ion

* Corresponding author. E-mail: hammond@mit.edu. Tel.: 617-258-7577.

(1) Larminie, J.; Dicks, A. *Fuel Cell Systems*; Wiley: New York, 2000.
(2) Kissa, E. *Dispersion*; Marcel Dekker: New York, 1999.
(3) Gottesfield, S.; Zawodzinski, T. *Adv. Electrochem. Sci. Eng.* **1997**, *5*, 195−301.
(4) Glipa, X.; Hograth, M. Department of Trade and Industry (U.K.) homepage http://www.dti.gov.uk/renewables/publications/pdfs/f02-00189.pdf, 2001.
(5) Skotheim; T. A.; Elsenbaumer, R. L.; Reynolds, J. R. *Handbook of Conducting Polymers*; Marcel Dekker: New York, 1998.
(6) Rubinson, J. F.; Mark, H. B., Jr. *Conducting Polymers and Polymer Electrolytes: From Biology to Photovoltaics*; Division of Colloid and Surface Chemistry, American Chemical Society: Washington, DC, 2002.
(7) Prasanna, C. *Conducting Polymers, Fundamentals and Applications: A Practical Approach*; Kluwer Academic Publishers: Dordrecht, The Netherlands, 1999.
(8) Rubner, M. F.; Cheung, J. H.; Fou, A. F. *Thin Solid Films* **1994**, *244*, 985.
(9) Rubner, M. F.; Fou, A. C. *Macromolecules* **1995**, *21*, 7115.
(10) Zhao, B. Z.; Neoh, K. G.; Kang, E. T. *J. Appl. Polym. Sci.* **2002**, *86*, 2099−2107.
(11) Grigore, L.; Petty, M. C. *J. Mater. Sci.: Mater. Electron.* **2003**, *14*, 389−392.
(12) Nishimura, H.; Iizuka, M.; Kuniyoshi, S.; Nakamura, M.; Kudo, K.; Tanaka, K. *Electron. Commun. Jpn. II: Electron.* **2004**, *87*, 18−25.
(13) Lu, W.; Fadeev, A. G.; Qi, B. H.; Mattes, B. R. *J. Electrochem. Soc.* **2004**, *151*, H33−H39.
(14) Bormashenko, E.; Pogreb, R.; Sutovski, S.; Shulzinger, A.; Sheshnev, A.; Gladkikh, A. *Synth. Met.* **2003**, *139*, 321−325.
(15) Rubner, M. F.; Stockton, W. B. *Macromolecules* **1997**, *30*, 2717−2725.
(16) Ferreira, M.; Huguenin, F.; Zucolotto, V.; da Silva, J. E. P.; de Torresi, S. I. C.; Temperini, M. L. A.; Torresi, R. M.; Oliveira, O. N. *J. Phys. Chem. B* **2003**, *107*, 8351−8354.
(17) Huguenin, F.; Ferreira, M.; Zucolotto, V.; Nart, F. C.; Torresi, R. M.; Oliveira, O. N. *Chem. Mater.* **2004**, *16*, 2293−2299.
(18) Park, M. K.; Onishi, K.; Locklin, J.; Caruso, F.; Advincula, R. C. *Langmuir* **2003**, *19*, 8550−8554.
(19) Sarkar, N.; Ram, M. K.; Sarkar, A.; Narizzano, R.; Paddeu, S.; Nicolini, C. *Nanotechnology* **2000**, *11*, 30−36.
(20) Stepp, J.; Schenkman, J. B. *J. Electrochem. Soc.* **1997**, *144*, L155-L157.
(21) Tian, S. J.; Baba, A.; Liu, J. Y.; Wang, Z. H.; Knoll, W.; Park, M. K.; Advincula, R. *Adv. Funct. Mater.* **2003**, *13*, 473−479.
(22) DeLongchamp, D. M.; Hammond, P. T. *Adv. Funct. Mater.* **2004**, *14*, 224−232.
(23) Decher, G.; Hong, J. D.; Schmitt, J. *Thin Solid Films* **1992**, *210/211*, 831−835.
(24) Arys, X.; Jonas, A. M.; Laschewsky, A.; Lagras, R. *Supramolecular Polymers*; Ciferri, A., Ed.; Marcel Dekker: New York, 2000; pp 505−564.
(25) Bertrand, P.; Jonas, A. M.; Laschewsky, A.; Lagras, R. *Macromol. Rapid Commun.* **2000**, *21*, 319−348.

10.1021/cm051335o CCC: $33.50 
Published on Web 12/06/2005

exchange[27−30] and ion conduction,[31−33] (iii) potential for induced porosity[34,35] and swellability,[36−38] (iv) tailored film thickness,[23−25] and (v) nonlithographic micropatterning.[39−42] Many researchers have been successful in making LBL thin films from conducting polymers such as polyaniline (PANi) and polypyrrole (PPy) in conjunction with polyanions such as poly(styrene sulfonate) (SPS), poly(acrylic acid) (PAA), and poly(2-acrylamido-2-methyl-1-propane sulfonic acid) (PAMPS)[43] and neutral polymers such as poly(ethylene oxide) (PEO), polyacrylamide (PAAm), and poly(vinyl alcohol) (PVA).[15] Electronic conductivities reported by most researchers for such films have ranged from 0.1 to 80 S $cm^{-1}$.[8,9,15,18,26] A major problem shared in previous work was the long-term stability of the assembled LBL film and the gradual degradation of its electronic conductivity.[8,10,15−18,22,26,43] Degradation in conductance was attributed to the loss of acidity due to either leaching or volatility of the dopant that renders the amine sites weakly protonated. However, catalyst loading for electrochemical reactive electrodes and induced porosity for enhanced ionic transport in LBL conducting thin films have not yet been attempted. Here, we investigate the potential use of the LBL technique to create composite polymeric thin film membranes that are both ionically and electronically conductive, as well as catalytically active.

Unlike the standard fabrication of fuel-cell electrodes where platinum powder is poured into a graphite slurry,[1,3,4] different approaches must be taken to load platinum into an LBL film.[44−48] Here, we investigate three different methods of platinum incorporation: reductive precipitation of a platinum salt complexed within the LBL film, polyelectrolyte colloidal platinum stabilization followed by LBL adsorption, and direct alternating adsorption of a positively charged polyaniline/platinum powder dispersion. In each method, polyaniline (PANi) was used as a conducting polymer with three selected polyanions of poly(acrylic acid) (PAA), poly(acrylate-*co*-acrylamide) (PAA-*co*-AAm), and poly(2-acrylamido-2-methyl-1-propane sulfonic acid) (PAMPS) (Figure 1a), and platinum was introduced as either a stabilized colloid, a salt (i.e., $H_2PtCl_6$) precursor, or a pure powder. The amount and nature of the incorporated platinum in the multilayers were analyzed by optical microscopy, scanning electron microscopy (SEM), SEM−X-ray analysis, and FTIR spectroscopy.

Among the three polyanions tested, PANi/PAA-*co*-PAAm exhibited the most promising morphology, and its electrochemical properties were characterized. Here, we report a relatively high and stable electronic conductivity, which is necessary for high passage of electrons to the outer circuit, and an ionic conductivity of approximately $10^{-5}$ S $cm^{-1}$, a value suitable for ultrathin supported electrodes. The catalyst loading in these films was tested by X-ray and SEM analysis and measuring the electrode potential generated by the PANi/PAA-*co*-PAAm electrode. Each of the properties measured are critical to the potential final applications of interest, including micropower galvanic and fuel cells and macro- and microarray detectors.

## Experimental Procedure

**Chemicals and Instrumentation.** The polyelectrolytes used were taken from the group consisting of poly(styrene sulfonic acid, sodium salt) (SPS, MW = 70 000), poly(diallyldimethylammonium chloride) (PDAC, MW = 240 000), linear poly(ethyleneimine) (LPEI, MW = 25,000), poly(acrylic acid) (PAA, MW = 90 000), and poly(acrylic-*co*-acrylamide acid, sodium salt) (PAA-*co*-AAm, MW = 10 000 000, 40% carboxy), all from Polysciences Inc. Poly(2-acrylamido-2-methyl-1-propane sulfonic acid) (PAMPS, 2 000 000), polyaniline (emeraldine base) (PANi, MW = 100 000) (Figure 1a), 1 methyl-2-pyrrolidonine, hydrogen hexachloroplatinate, and the sodium salts of citrate and borohydride were all from Aldrich. Potassium hexacyanoruthenate was from Alfa-Aesar, and (±)-camphore-10-sulfonic acid($\beta$) was from Fluka. Hydrogen (grade 4.7) and nitrogen (grade 5) purge gases were from BOC.

Platinum powder (average size ≈ 0.15−0.45 $\mu$m) and platinum and gold plates were all from VWR (Alfa Aesar). Nucleopore membranes (0.1-$\mu$m pore size) were purchased from SPI supplies. The surface roughness and thickness of the electrode were measured using a surface profiler from Tencor Instruments (type P-10). Scanning electron microscopy (SEM) (JEOL 5910/SEM), X-ray quantitative analysis, high-resolution scanning electron microscopy (JEOL 6320 FEGSEM), and X-ray photoelectron spectroscopy (XPS) were used to examine the topography, catalyst loading, and surface structure of the electrodes. A ZetaPALS instrument ($\zeta$ potential analyzer) from Brookhaven Instrument Co. was used to measure the $\zeta$ potential and mobility that characterize the surface charge and quality of the colloidal dispersions. Substrates were plasma-etched under vacuum with a plasma cleaner/sterilizer (PDC-32G), and IR spectra were recorded using a Nicolet 550 SeriesII FTIR spectrometer. A model 276 potentiostat from EG&G Princeton Applied Research was used for electrochemical and ohmic measurements, and a type SI 1260 ac impedance analyzer from Solartron Inc. was used to measure ion conductivity.

(26) Li, W.; Hooks, D. E.; Chiarelli, P.; Jiang, Y.; Xu, H.; Wang, H. *Langmuir* **2003**, *19*, 4639−4644.
(27) Farhat, T. R.; Schlenoff, J. B. *Langmuir* **2001**, *17*, 1184−1192.
(28) Farhat, T. R.; Schlenoff, J. B. *J. Am. Chem. Soc.* **2003**, *125*, 4627−4636.
(29) Harris, J. J.; DeRose, P. M.; Bruening, M. L. *J. Am. Chem. Soc.* **1999**, *121*, 1978.
(30) Bruening, M. L.; Miller, M. D.; Harris, J. J.; Stanton, B. W. *Langmuir* **2003**, *19*, 7038−7042.
(31) DeLongchamp, D. M.; Hammond, P. T. Ph.D. Thesis, Massachusetts Institute of Technology, Cambridge, MA, 2003.
(32) DeLongchamp, D. M.; Hammond, P. T. *Chem. Mater.* **2003**, *15*, 1165−1173.
(33) Tokuhisa, H.; Hammond, P. T. *Adv. Funct. Mater.* **2003**, *13*, 831−839.
(34) Rubner, M. F.; Barret, C. J.; Chan, J. J.; Pal, A. J.; Mayes, A. M.; Mendelsohn, J. D. *Langmuir* **2000**, *16*, 5017−5023.
(35) Caruso, F.; Fery, A.; Scholer, B.; Cassagneau, T. *Langmuir* **2001**.
(36) Farhat, T.; Yassin, G.; Dubas, S. T.; Schlenoff, J. B. *Langmuir* **1999**, *15*, 6621−6623.
(37) Dubas, S. T.; Schlenoff, J. B. *Macromolecules* **1999**, *32*, 8153−8160.
(38) Losche, M.; Schmitt, J.; Decher, G.; Bouwman, W. G.; Kjaer, K. *Macromolecules* **1998**, *31*, 8893.
(39) Clark, S. L.; Hammond, P. T. *Langmuir* **2000**, *16*, 10206−10214.
(40) Hammond, P. T.; Zheng, H. P.; Rubner, M. F. *Langmuir* **2001**, *18*, 4505−4510.
(41) Hammond, P. T. *Adv. Mater.* **2004**, *16*, 1271−1293.
(42) Park, J.; Hammond, P. T. *Adv. Mater.* **2004**, *16*, 520.
(43) DeLongchamp, D. M.; Hammond, P. T. In *Chromogenic Phenomena in Polymers*; 2005; Vol. 888; pp 18−33.
(44) Cohen, R. E.; Rubner, M. F.; Wang, T. C. *Chem. Mater.* **2003**, *15*, 299−304.
(45) Halaoui, L. I.; Ghannoum, S.; Xin, Y.; Jaber, J. *Langmuir* **2003**, *19*, 4804−4811.
(46) Krass, H.; Papastavrou, G.; Kurth, D. G. *Chem. Mater.* **2003**, *15*, 196−203.
(47) Mallouk, T. E.; Feldheim, D. L.; Crabar, K. C.; Natan, M. J. *J. Am. Chem. Soc.* **1996**, *118*, 7640−7641.
(48) Murray, R. W.; Hicks, J. F.; Seok-Shon, Y. *Langmuir* **2002**, *18*, 2288−2294.

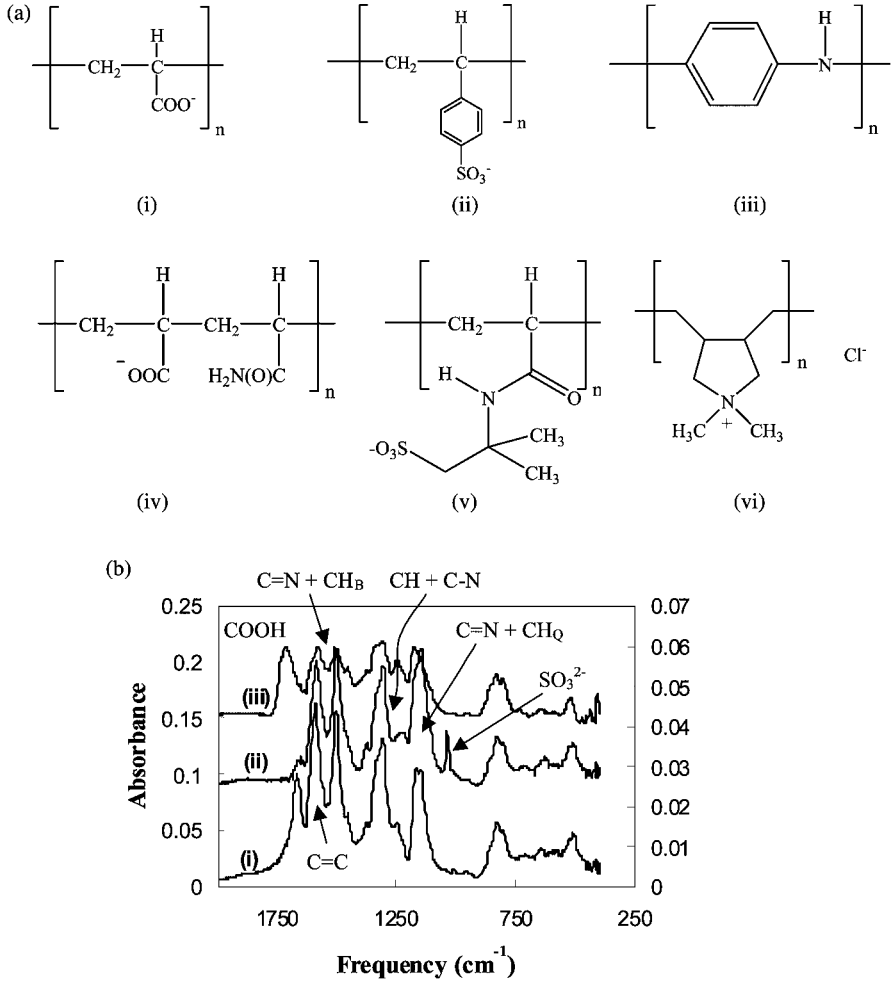


**Figure 1.** (a) (i) Poly(acrylic acid) (PAA), (ii) poly(styrene sulfonic acid, sodium salt) (SPS), (iii) polyaniline (emeraldine base) (PANi), (iv) poly(acrylic-*co*-acrylamide acid, sodium salt) (PAA-*co*-AAm), (v) poly(2-acrylamido-2-methyl-1-propane sulfonic acid) (PAMPS), (vi) poly(diallyldimethylammonium chloride) (PDAC). (b) FTIR spectra of (i) PANi/poly(acrylic acid-*co*-acrylamide) (PAA-*co*-PAAm), (ii) PANi/PAMPS, (iii) PANi/poly(acrylic acid). LBL films containing PAA-*co*-PAAm and PAA showed a strong carbonyl stretch of the COOH group at 1669 and 1717 $cm^{-1}$, respectively. Those containing PAMPS showed a strong $SO_3^-$ stretch at ~1040 $cm^{-1}$ and a diffuse amide peak at 1660 $cm^{-1}$. Peaks at 1170 $cm^{-1}$ (C═N + $CH_Q$), 1310 $cm^{-1}$ (C−H or C−N), 1510 $cm^{-1}$ (C═N + $CH_B$), and 1590 $cm^{-1}$ (C═C) are common to all films and characterize the PANi IR spectrum. $T$ = 23 °C, RH ≈ 10%.

**Electrode Assembly.** Platinum loading into the LBL polyaniline matrix was tested using three different methods that are described in detail later in this section.

*Substrate Preparation.* For FTIR analysis, silicon wafers [single-sided polished Si(100) wafers that were n-type P-doped (~400-$\mu$m thickness) and more than 60% transmissive to IR radiation] were washed with pure water and ethanol and then plasma-etched under vacuum for 3 min. FTIR analysis of these wafers was used for qualitative or relative measurements. Quantitative measurements were confined to X-ray SEM only. The LBL composite membrane was prepared as described previously,[49] with a polyanionic final layer (i.e., PAMPS). Plastic polystyrene strips were cut from Permanox PS slides and directly plasma-etched under vacuum for 5 min. Nucleopore membranes were mildly etched for only 1.5 min to prevent damage from prolonged plasma exposure. Gold substrates, with thicknesses of ~1500 Å, were prepared by evaporating gold nuggets from a tungsten crucible at a pressure of $10^{-6}$ Torr onto a masked Nucleopore membrane using a metal evaporator. The gold pattern was plasma-etched for 5 min, and the sample was then subjected to 2 h of deposition in a 10.0 mM solution of SPS to render the surface negatively charged. After treatment, all substrates were directly dipped into a solution containing a positively charged polyaniline colloid at pH ~2.5 for 30 min to assemble a complete monolayer.

*Preparation of the Polyelectrolyte Solutions.* The cationic polyaniline solution was prepared by sifting 0.07−0.1 g of PANi powder in a 175 mesh sieve followed by sifting in a finer 325 mesh sieve where the fine powder was collected over 30.0 mL of 1-methyl 2-pyrrolydonine under continuous stirring. Next, the dark-blue PANi solution was sonicated for 2 h and then acidified by adding 60.0 mL of camphor sulfonic acid at pH ~2.3, causing it to turn dark-green. In all experiments, the concentrations ranged between 5.0 and 8.0 mM.[8,9,15,45] The following polyanionic solutions were adsorbed in alternation with a PANi solution of pH 2.5 in separate dipping experiments [polyanion (concentration)/pH]: SPS (10.0 mM)/2.5, PAA (10.0 mM)/4.0, PAA (10.0 mM)/6.0, PAA-*co*-PAAm (2.0 mM)/4.0, PAA-*co*-PAAm (2.0 mM)/6.0, and PAMPS (5.0 mM)/2.5.

*LBL Deposition.* In all methods, the LBL deposition technique was used to form conducting ultrathin electrodes. After a monolayer of PANi had been formed, as described in the Substrate Preparation section above, the substrate was rinsed four times in pH 2.5 pure water for durations of 2, 1, 1, and 1 min, respectively. The rinsing stage was followed by 10 min of deposition from a polyanionic solution adjusted to pH 4 to assemble nonporous films and pH 6 to assemble porous films. Again, the first bilayer was then rinsed four separate times in pure water at pH 4.0 or 6.0 for durations of

(49) Farhat, T. R.; Hammond, P. T. *Adv. Funct. Mater.* **2005**, *15*, 945−954.

2, 1, 1, and 1 min, respectively. After the first bilayer, the substrate was deposited in the PANi solution for 15 min only. Unless stated, a total of 40 bilayers of polyanion/PANi were deposited on the various substrates to assemble LBL PANi/polyanion electrodes.

*Methods Used to Load the Platinum Catalyst.* (i) Polyelectrolyte Colloidal Platinum Stabilization. Colloidal platinum nanoclusters were synthesized by refluxing a mixture of $H_2PtCl_6$ and sodium citrate (wt/wt ratio = 1:30) in a 20.0 mM solution of PAA (or SPS) for 2 h.[45,47,48,50,51] After being refluxed, the golden-brown Pt− colloid material was centrifuged for 5 min, repeatedly decanted, and washed with pure water to remove any free PAA (or SPS) and citrate. The concentrate was then diluted with pure water to obtain a 5.0−10.0 mM PAA platinum colloidal solution.

(ii) Reductive Precipitation of the Platinum Salt inside the LBL Film. Initially, a fully assembled 40-bilayer PANi/polyanion LBL film was soaked in a 10.0 mM $H_2PtCl_6$ solution for 10.0 min. The dosing process was followed by rinsing the LBL film in pure water (pH 2.5) to remove any remnants of $PtCl_6^{2-}$ that did not complex within the LBL matrix. The $PtCl_6^{2-}$ salt that was trapped inside the film was reduced to platinum black clusters by soaking in 2.0 mM $NaBH_4$ solution adjusted to pH 4. The $NaBH_4$ solution is basic, which can dedope the films; however, films were then acid-treated and placed in 20 mM sulfuric acid during the electrode potential measurements to restore their conductivity. In a separate experiment, the incorporation of the IR-active $Ru(CN)_6^{3-}$ salt inside the LBL film was monitored using FTIR spectroscopy.

(iii) Polyaniline Solution/Platinum Powder Dispersion. In this method, a stable dispersion of cationic PANi/platinum powder was prepared and LBL-assembled with polyanionic solutions such as PAA-*co*-PAAm and PAMPS. The preparation of the PANi/platinum powder dispersion is similar to the technique described in the Preparation of the Polyelectrolyte Solutions section for PANi. However, in this case, the camphor sulfonic acid solution was impregnated at a concentration of 0.1 g/100.0 mL with platinum powder having an average size of 0.2 $\mu$m. The mixture was subjected to 2 h of sonication, and again 60.0 mL of this dispersion was quickly transferred to the organic PANi solution. It should be noted that larger platinum particulates were subject to quick sedimentation. The resulting PANi/platinum powder mixture was further sonicated for 1 h to obtain the final dispersion.

*Electrochemical Measurements.* Electrode potentials of half-cells composed of either a pure platinum, a pure gold, or a platinum-catalyzed PANi/PAA-*co*-PAAm electrode in a 20 mM $H_2SO_4/H_2$-purged electrochemical cell were compared. The electrode potential (recorded as an open-circuit potential, OCP) of a half-cell was measured vs a saturated calomel electrode (SCE) using a voltmeter and a potentiostat in the open-circuit mode. Electronic conductivities, for a particular film thickness (e.g., 3.0 $\mu$m), were calculated from resistance or impedance measurements where the area of contact was equal to 0.06 $cm^{-2}$ (i.e., 2 mm × 3 mm) and the distance between the contact electrodes was 1 cm. All conductance measurements were made using a potentiostat, an ac impedance analyzer, and an ohmmeter. Prior to ac impedance analysis of ionic conductance, LBL films of PANi/PAA-*co*-PAAm were treated with 0.5 M NaCl in pH 8 buffer for 1 h before measuring their impedance.

## Results and Discussion

**Assembly of Porous and Nonporous Films.** Polyelectrolyte multilayer thin films were assembled with PANi and three different co-polyanions: PAA, PAA-*co*-PAam, and PAMPS. Assembly with all three polyanions was successful, leading to stable multilayer thin films. The pH of the PANi solution during assembly was maintained at 2.5 to achieve a relatively high charge density along the backbone and maintain the doped form of the PANi polymer. The pH of the polyanion solutions was adjusted within a range such that the carboxylic acid groups on weak polyelectrolytes were partially charged, thus promoting the growth of thicker films with higher innate ionic conductivity.[32] The pH of the strong polyanion, PAMPS, was simply maintained at pH 2.5 to match the conditions of the PANi solution.

In general, a 40-bilayer LBL PANi (5.0 mM, pH 2.5)/PAA (10.0 mM, pH 4.0), PAA-*co*-PAAm (2.0 mM, pH 4.0), or PAMPS (5.0 mM, pH 2.5) film exhibited a relatively large thickness of 3 $\mu$m (i.e., 750 Å per bilayer) and a characteristic surface roughness of ∼30−50 nm. LBL PANi film assembly was verified by FTIR spectroscopy [Figure 1b (**i**−**iii**)]. LBL films containing PAA-*co*-PAAm and PAA exhibited a strong carbonyl stretch of the carboxylate group at 1669 and 1717 $cm^{-1}$, respectively. The PAMPS IR signal revealed a strong sulfonate stretch at ∼1040 $cm^{-1}$ and a diffuse amide peak at 1660 $cm^{-1}$. Peaks at 1170 $cm^{-1}$ (C═N + $CH_Q$ bend in the Q ring), 1310 $cm^{-1}$ (C−H or C−N), 1510 $cm^{-1}$ (C═N + $CH_B$ bend in the B ring), and 1590 $cm^{-1}$ (C═C) were common to all films and characterize the PANi IR spectrum.[52] Scanning electron microscopy (SEM) revealed that different surface textures were obtained when different polyanions were assembled with PANi, as shown in Figure 2, for which PANi was LBL-deposited with PAA and PAMPS, respectively. All PANi/PAA or PANi/PAA-*co*-PAAm LBL films exhibited a waxy soft texture (Figure 2a), whereas PANi/PAMPS films were hard and brittle and exhibited cracks specifically when assembled on hard substrates [e.g., Si(100) wafer] (Figure 2b). In addition, films containing the weak polyanions, specifically PANi/PAA and PANi/PAA-*co*-PAAm, formed porous structures because of the changes in pH conditions during assembly. For example, when the PANi colloidal solution and its rinse baths were buffered at pH 2.5 and the PAA-*co*-PAAm (or PAA) solution and its rinse baths were buffered at pH 6.0, the resulting LBL PANi film were extremely porous (Figures 2a and 3a,b). No porous structure was detected when PAA-*co*-PAAm (or PAA) solution and its rinse baths were buffered at pH 4 (Figure 3c; Figure 1 Supporting Information). Spinodal decomposition and pore formation is a well-reported phenomenon that occurs in some LBL films[34,35,53] when initiated by changes in the pH or salt concentration after assembly. For example, when the partially charged polyelectrolytes of LPEI (pH 4) and PAA (pH 4) are assembled as an LBL composite membrane on a Nucleopore filter and then soaked in pH 2 solution, the membrane turns from clear to opaque white, indicating the formation of pores as a result of phase separation of the −COOH groups in PAA.[34,35,54] In the PANi/PAA or PANi/PAA-*co*-PAAm systems, pore formation

(50) Schmitt, J.; Decher, G.; Dressick, W. J.; Brandow, S. L.; Geer, R. E.; Shashidhar, R.; Calvert, J. M. *Adv. Mater.* **1997**, *9*, 61−65.
(51) Sun, S. e. a. *J. Phys. Chem. B* **2003**, *107*, 5419−5425.
(52) Arora, M.; Luthra, V.; Singh, R.; Gupta, S. K. *Appl. Biochem. Biotechnol.* **2001**, *96*, 173−181.
(53) Lowman, G.; Tokuhisa, H.; Lutkenhaus, J.; Hammond, P. T. *Langmuir* **2004**, *20*, 9791−9795.
(54) Lowman, G.; Hammond, P. T. *Small* **2005**, *1*, 1070−1073.

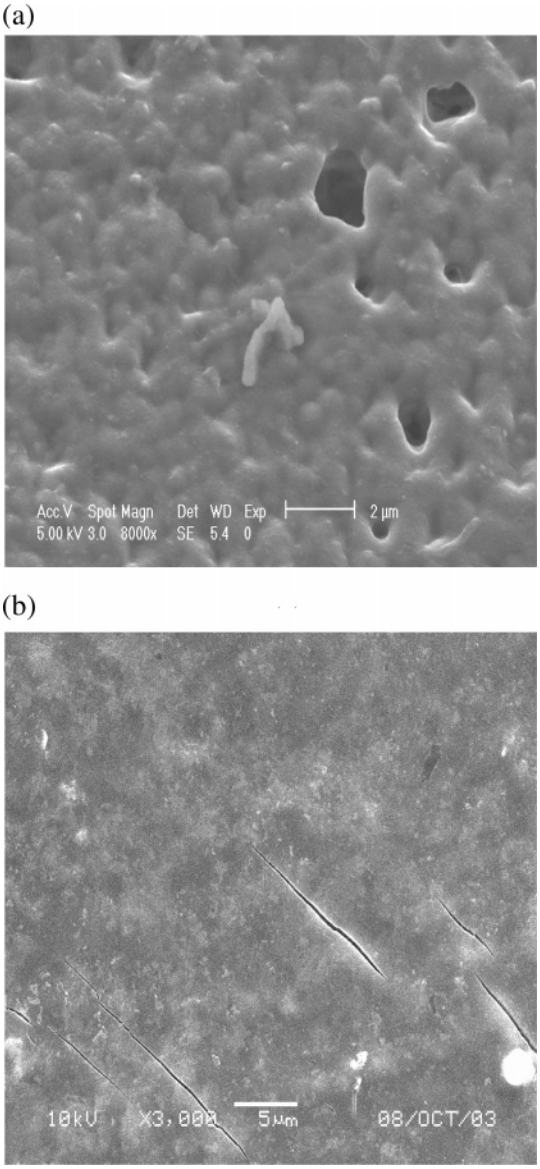


**Figure 2.** Scanning electron microscopy image of layer-by-layer films of (a) PANi (pH 2)/poly(acrylic acid) (pH 6), resolution = 2.0 $\mu$m, $V$ = 5.0 kV and (b) PANi/poly(2-acrylamido-2-methyl-1-propane sulfonic acid), resolution = 5.0 $\mu$m, $V$ = 10.0 kV. The surface topology showed different surface textures when different polyanions were assembled with PANi. All PANi/PAA and PANi/PAA-*co*-PAAm LBL films exhibited a waxy soft texture, whereas PANi/PAMPS were brittle.

occurs at pH 6 when the −COO − groups phase separate from the neutral polyaniline backbone. Other effects to consider are polyelectrolyte-on-polyelectrolyte coiling and desorption.[55] Polyelectrolytes such as PAA or PAA-*co*-PAAm are flexible but, if combined with the stiff PANi backbone, would induce polymer coiling. Any complex formed can either remain on the surface or desorb, and in the process, a network-like structure is formed. Whether it is phase separation or a coiling−desorption effect, it is evident that a porous structure developed after the first few bilayers were deposited, as shown in Figure 4 (Figure 2 Supporting Information). Under optical microscopy, the first and second bilayers (not shown) exhibited green islands of PANi/PAA-*co*-PAAm (or PAA) scattered randomly on the surface. With more bilayer deposition, the islands eventually connect at the sixth bilayer to produce the base of a porous structure (Figure 4). Among the three types of PANi/polyanion electrodes studied, the PANi/PAA-*co*-PAAm electrode exhibited the best film uniformity, as well as the porous structure most conducive to ion transport, prompting us to study its catalyst loading and electrochemical characteristics.

**Platinum Loading.** A 40-bilayer PANi/PAA-*co*-AAm LBL electrode was loaded with platinum by reductive precipitation of the platinum salt $PtCl_6^{2-}$ inside the LBL film using $NaBH_4$ (pH 4) as the reductant. This general approach of using free charged groups to complex and reduce metal salts has been demonstrated to be successful for the introduction of a number of metals and metal oxides within multilayer thin films, including silver and iron oxides.[56−60] The 40-bilayer film was soaked in the platinum salt solution for at least 10 min to give the $PtCl_6^{2-}$ salt enough time to permeate and complex with the ion-pair sites inside the LBL film.[27,36] The complexation process, known as "reluctant ion exchange", is an ion-exchange process that occurs only in fully or partially ionized LBL films where ion transport is a function of the charge of the ion and any supporting salt. The higher the charge, the more slowly the ions diffuse across an LBL film.[27,28] Consequently, a PANi/PAA-*co*-AAm LBL film allows the singly charged $BH_4^-$(aq) ions to permeate much more rapidly inside the LBL film before the doubly charged $PtCl_6^{2-}$ ions can start to leach out. This effect allows the reduction of most of the $PtCl_6^{2-}$ salt to platinum black. The PANi electrode was checked for platinum content using SEM X-ray analysis (Figure 5a). A strong chloride peak at 2.63 keV indicated that not all of the platinum salt $PtCl_6^{2-}$ had been reduced to platinum. Taking into consideration the atomic number of each element, quantitative analysis of the energy-dispersive spectrum indicated that the ratio of platinum to chlorine is 3:1 (i.e., ratio of the local mass fraction). Therefore, 8% of the platinum content is in the salt form, and the remainder is platinum black. The X-ray signal of the same sample was compared to that of a commercial E-TEK electrode (~0.5 mg cm$^{-2}$ according to manufacturer) (Figure 5b), where the LBL PANi electrode measured a moderately high platinum content of 0.3 mg cm$^{-2}$, verifying that the dosing procedure is very effective in loading platinum inside the PANi/PAA-*co*-AAm electrode matrix. Dosing by reluctant ion exchange[27,28] was also verified by soaking every bilayer of PANi/PAA-*co*-AAm in a solution of the IR-active ruthenium salt [$Ru(CN)_6^{3-}$] and monitoring the C≡N stretch at 2070 cm$^{-1}$ (Figure 6a). It is evident the IR signal is nearly 7 times stronger for the ninth compared to the third bilayer. The increase in the ruthenium salt content with the number of bilayers deposited is illustrated in the

(55) Park, J.; Hammond, P. T. *Macromolecules*, manuscript submitted.

(56) Lee, D.; Rubner, M. F.; Cohen, R. E. *Chem. Mater.* **2005**, *17*, 1099−1105.
(57) Wang, T. C.; Chen, B.; Rubner, M. F.; Cohen, R. E. *Langmuir* **2001**, *17*, 6610−6615.
(58) Wang, T. C.; Rubner, M. F.; Cohen, R. E. *Langmuir* **2002**, *18*, 3370−3375.
(59) Wang, T. C.; Rubner, M. F.; Cohen, R. E. *Chem. Mater.* **2003**, *15*, 299−304.
(60) Yang, S. Y.; Lee, D.; Cohen, R. E.; Rubner, M. F. *Langmuir* **2004**, *20*, 5978−5981.

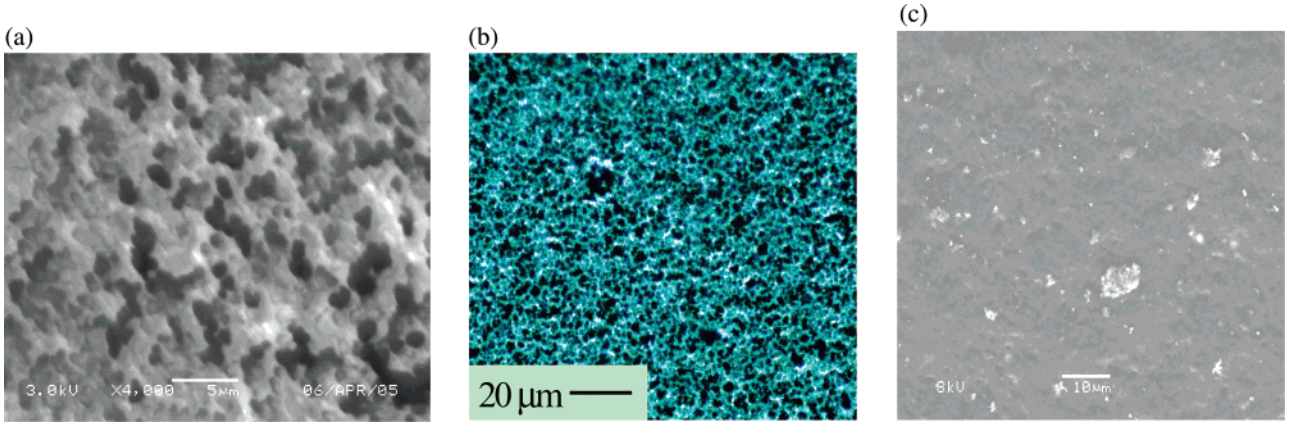


**Figure 3.** Scanning electron microscopy (SEM) and optical microscopy (OM) images of layer-by-layer films of PANi/poly(acrylic acid-*co*-acrylamide) (PAA-*co*-PAAm) assembled under different pH conditions. (a) SEM image of PANi (pH 2.5), baths (pH 2.5), with PAA-*co*-PAAm (pH 6), baths (pH 6); resolution = 2.0 $\mu$m, $V$ = 3.0 kV. (b) OM image of the film in a at resolution = 20.0 $\mu$m. (c) SEM image of PANi (pH 2.5), baths (pH 4), with PAA-*co*-PAAm (pH 4), baths (pH 4); resolution = 10.0 $\mu$m, $V$ = 6.0 kV. The white scattered dots are platinum particles embedded using the polyaniline−platinum powder dispersion method.

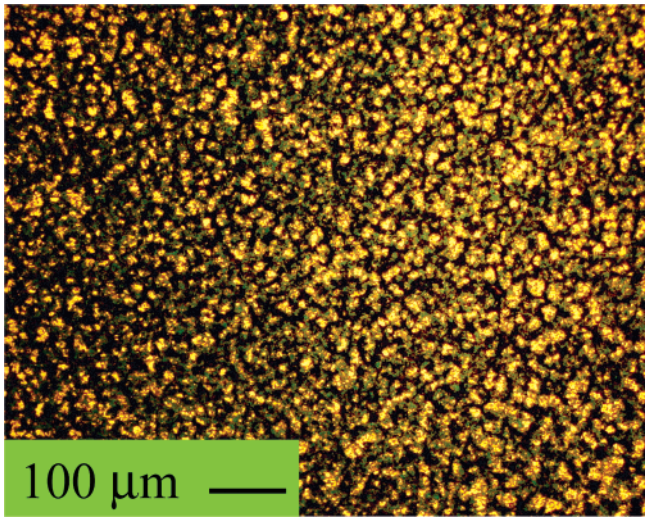


**Figure 4.** Optical microscopy images of PANi/PAA-*co*-PAAm LBL film growth under a pH regime of PANi (pH 2.5), baths (pH 2.5), with PAA-*co*-PAAm (pH 6), baths (pH 6); resolution = 100.0 $\mu$m. Evidence for the development of a porous structure when the first few bilayers were deposited is illustrated. The islands connected at the onset of deposition of the sixth bilayer to produce the base of a porous structure.

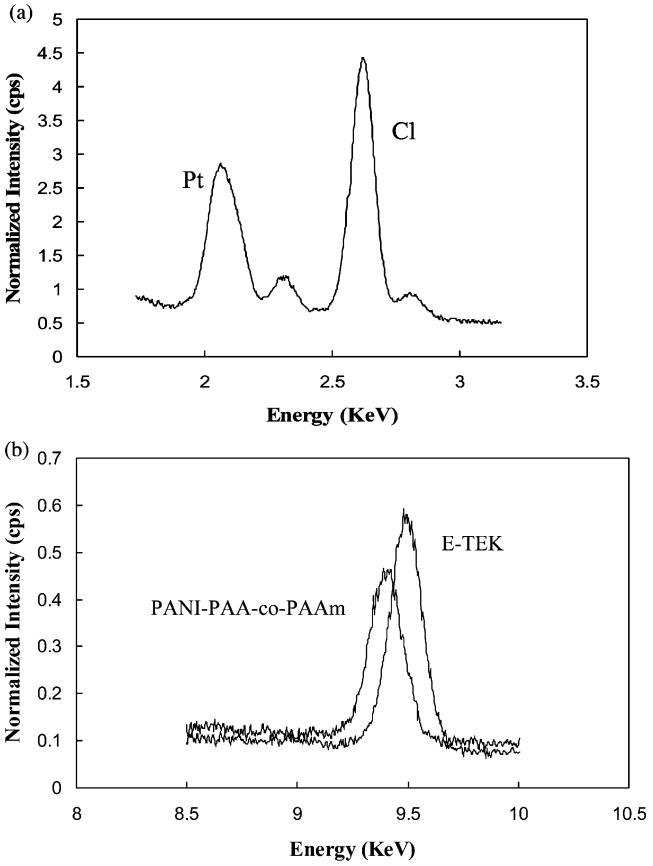


**Figure 5.** (a) Polyaniline/poly(acrylic acid-*co*-acrylamide) LBL electrode checked for platinum content using SEM X-ray analysis. A strong chloride peak at 2.63 keV indicates that not all of the platinum salt $PtCl_6^{2-}$ has been reduced to platinum. Quantitatively, 8% of the platinum content is in the salt form, and 92% is platinum black. (b) Same sample compared to an X-ray signal from a commercial E-TEK electrode (~0.5 mg cm$^{-2}$) exhibited a moderately high platinum content of 0.3 mg cm$^{-2}$. Scanned area at resolution = 100 $\mu$m, $V$ = 30 kV, spot size = 52, aperture = 3, cps ≈ 60 K.

plot of Figure 6b. Permeation of the $Ru(CN)_6^{3-}$ ions is similar to $PtCl_6^{2-}$ or $Fe(CN)_6^{3-}$ ions that undergo reluctant ion exchange and then complex to the ion-pair sites in the bulk of the film.

Platinum loading utilizing colloidal stabilization of platinum was done using polyelectrolytes of PAA or SPS to stabilize the synthesized platinum clusters (size ≈ 5 nm), thus making a polyanionic colloidal solution. $\zeta$ potentials of the stabilized clusters were $\zeta = -55.2$ mV for Pt/PAA colloid and $\zeta = -46.4$ mV for the Pt/SPS colloid. Values that are more negative than −45 mV indicate very good electrosteric stability[2] imposed by the negatively charged polymer segments coating the platinum clusters. The polyanionic colloidal solutions were LBL-assembled with acidified cationic PANi (pH 2.5) solution to form thin LBL PANi conducting films. This method yielded an extremely low platinum content (<0.005 mg cm$^{-2}$). The low platinum content was attributed to thinner PANi/polyanion films (thickness < 0.1 $\mu$m) due to a possible drop in the charge density of the polyanion as it complexes to the platinum colloid, making it difficult for the weakly charged PANi to assemble. Another possibility is continuous desorption of the colloidal particles from the film surface into the PANi solution during assembly. Finally, the third method utilizing polyaniline−platinum powder dispersions made by prolonged sonication of platinum powder in polyaniline did assemble

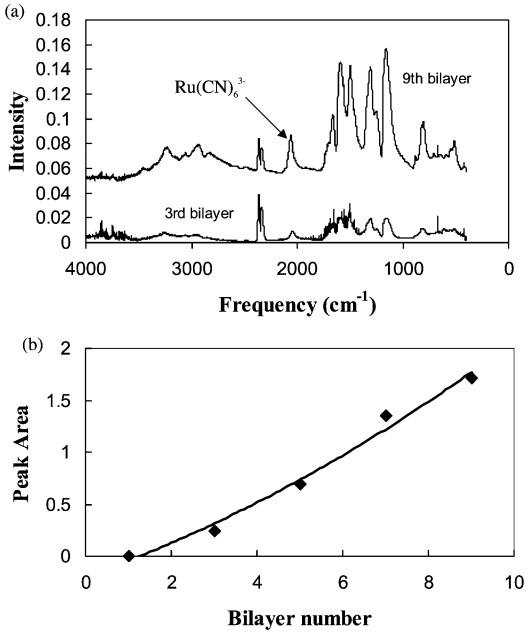


**Figure 6.** (a) FTIR spectra of the third and ninth bilayers of a polyaniline PANi/PAA-*co*-AAm LBL film showing a strong IR signal of the nitrile group (−C≡N) at 2070 $cm^{-1}$ after being soaked in the IR-active ruthenium salt of $[Ru(CN)_6^{3-}]$. (b) Peak area of the nitrile [C≡N] stretch at 2070 $cm^{-1}$ vs bilayer number, illustrating an increase in the ruthenium salt content as the PANi LBL electrode thickness increases.

with PAMPS and PAA-*co*-AAm, but SEM indicated individually scattered platinum particulates over the surface (Figure 3c; Figure 1 Supporting Information). The latter method can be remedied by using platinum powder of nanometer size (i.e., 20−60 nm); however, because of its specialty market, the cost of the platinum colloid would significantly increase the total electrode costs using this approach. Of the three approaches described here, the first approach of ion exchange with Pt salts, followed by reduction to form Pt nanoparticles within the film, was the superior method. It should be pointed out that the other two methods might still hold merit for the incorporation of Pt or other metal or metal oxide systems. Key to achieving a high inorganic loading content would be an enhancement in the charge density of the resulting colloids through pH adjustments and choice of charged group and the use of nanoscale particles with controlled or limited aggregation. For this reason, we present these other two techniques as options that will be of interest for future studies.

**Electrochemical Properties.** In exploring electrode materials designed for fuel-cell and other electrochemical applications, the measurement of properties is essential. Measuring the ionic conductivity of electronically conducting pH-dependent thin films (e.g., PANi/SPS) is difficult because both factors can contribute to the overall impedance, as shown schematically in Figure 7a. It is obvious that there are two paths for the passage of charge, expressed as ionic and electronic conductance (or the measured impedance *Z*). In its simplest form, the two paths are illustrated by two Randel cells connected in parallel (Figure 7b) that represent ionic and electronic impedances. A parallel connection would yield a Nyquist plot of one semicircle from which it is difficult to discern which conduction process is a major contributor to the total impedance, $Z_T$. To determine which

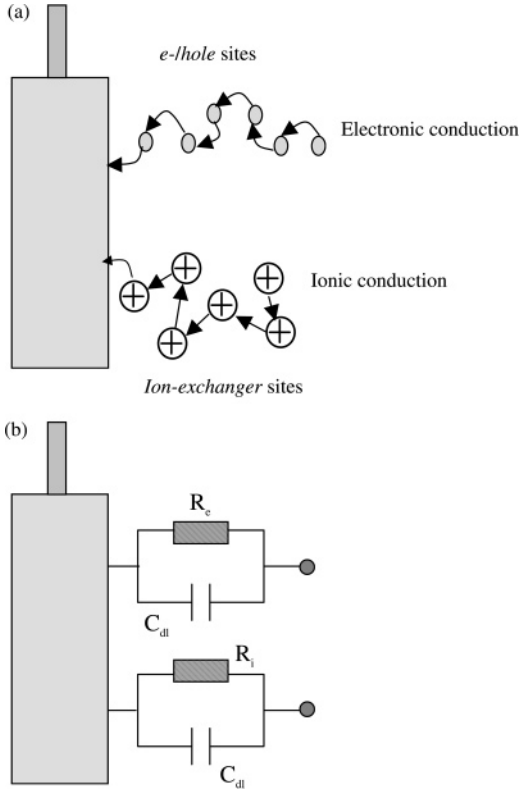


**Figure 7.** (a) Schematic showing two paths for the passage of charge expressed as ionic and electronic impedance. (b) Ionic and electronic conductances represented by two Randel cells connected in parallel. $R_e \equiv e^-$/hole charge-transfer resistance, $R_i \equiv e^-$/ion charge-transfer resistance, $C_{dl} \equiv$ double-layer capacitance.

factor is dominant, we considered the ionic conductivity in LBL films made from strong, nonconducting polyelectrolytes as a control.

It is known that the ionic conductivity in LBL films increases with humidity;[31,32,61] however, in LBL conducting polymer electrodes, humidity can increase both ionic and electronic conductivities. Ionic conductivity is increased by enhancing the ionic mobility across the water clusters within the bulk of the film, whereas higher electronic conductivity is achieved by trapping the hydronium ions that further dope the polymer. For this reason, the hydrophobic character of an LBL conducting film plays a critical role in the overall conduction process. LBL conducting polymer electrodes such as $(PANi/SPS)_n$ and polypyrrole $(PPY/SPS)_n$[9,15,45] are known to have high electronic conductivities ($0.1 < \sigma_e < 80$ S $cm^{-1}$) when dosed with strong acids such as HCl.[8,9,15] However, these electrodes are strongly hydrophobic, and hydrophobic LBL films such as PDAC/SPS exhibit very low ionic conductivities ($\sigma_i < 10^{-8}-10^{-9}$ S $cm^{-1}$) measured under acidic conditions. Hence, the only way the ionic conductivity can be independently measured in LBL PANi electrodes is to eliminate the electronic conductance by soaking the electrode in basic solutions to dedope the polymer, as explained later. Extremely low ionic conductivity is considered a drawback if these electrodes are to be used in electrochemical systems such as fuel cells. Consequently,

(61) DeLongchamp, D. M.; Hammond, P. T. *Abstr. Pap. Am. Chem. Soc. S22* **2001**, *136-PMSE, Part2.*

**Table 1.**

| technique | $\sigma_e$ (S cm$^{-1}$) at RH < 21% | $\sigma_e$ (S cm$^{-1}$) at RH > 80% |
|---|---|---|
| ac impedance | 1.15 | 1.94 |
| chronopotentiometry | 1.16 | 2.3 |
| ohmeter | 1.0 | 1.4 |

hydrophilic anions such as PAA or PAA-*co*-PAAm are substituted for SPS to promote ionic conduction.

*Ionic Conductivity.* To improve ionic conduction, SPS was replaced by the hydrophilic PAA, PAMPS, or PAA-*co*-AAm polyanions. It was mentioned in the experimental procedure in the Preparation of the Polyelectrolyte Solutions section that camphor sulfonic acid has to be introduced into the PANi solution during LBL assembly as part of the doping procedure. In an effort to minimize the contribution from electronic conductance, LBL films of PANi/PAA-*co*-PAAm were soaked in a basic solution of pH 8.0 for more than 1 h to deprotonate the amine groups in the PANi polymer backbone. Electrochemical impedance verified that the conductivity of the samples dropped from ~0.5 S cm$^{-1}$ before basic treatment to $3.6 \times 10^{-5}$ S cm$^{-1}$ after dosing with 0.5 M NaCl/pH 8.0 solution. Moreover, the ohmeter read a resistance above 2.0 MΩ, which is an indication of negligible electronic conductance. It is thus reasonable to conclude that the inherent ionic conductivity of the LBL matrix is on the order of $10^{-5}$ S cm$^{-1}$, which is considered moderately high in LBL films where the salt ions are considered the major contributor as in this case. Because the remnant of proton propagation across the PANi polymer backbone is also possible in these LBL thin film systems, under acidic conditions, the ionic conductivity is expected to be higher as a result of a larger population of protons.

*Electronic Conductivity.* LBL conducting polymer electrodes of PANi/PAA-*co*-AAm exhibited electronic conductivities, $\sigma_e$, that ranged from 0.5 to 2.3 S cm$^{-1}$. Our values are similar to those reported previously[8,9,15,18,26] (i.e., 0.1−4.0 S cm$^{-1}$). The characteristic $\sigma_e$ value of PANi/PAA-*co*-AAm electrodes ranged from 1.0 to 2.3 S cm$^{-1}$ as measured using ac impedance, chronopotentiometry, and an ohmmeter under ambient conditions (i.e., no inert atmosphere). $\sigma_e$ values for the PANi/PAA-*co*-AAm electrodes are listed in Table 1. The conductivity of LBL PANi films went up by 1.2 S cm$^{-1}$ as the humidity and temperature were increased, an environment favored during fuel-cell operation. Humidity and temperature effects were monitored using ac impedance Nyquist plots. For example, in Figure 8, the magnitude of the impedance $|Z|$ decreased from an average of 9.5 to 6.8 kΩ as a result of a change in relative humidity (RH) from 19.5% to 82%. Increasing the temperature from 20 to 40 °C decreased $|Z|$ by ~2.3 kΩ. In another experiment, (Figure 3 Supporting Information), a 2.0-μA current passed through a PANi/PAA-*co*-AAm LBL electrode at 20% RH caused a voltage drop of 25 mV because of a 12.5 kΩ film resistance. When RH was increased to 99%, the film resistance dropped to 7.5 kΩ because of a higher electronic conductivity. A common problem that is shared by researchers working with LBL PANi electrodes is the degradation of $\sigma_e$ under ambient conditions. The main culprit is the volatility of the doping acids, which can eventually lead to deprotonation of the amine groups along the PANi backbone, thus shutting off the electron-hopping capability. Unexpectedly, the PANi/PAA-*co*-AAm LBL electrodes exhibited relatively good stability, evidenced by the fact that the voltage signal remained constant after 1 h (Figure 3 Supporting Information). Under ambient conditions, repeated checks of the electronic conductivity were made over many days, and a loss of only ~0.3 S cm$^{-1}$ was reported in most samples. The stability in electronic conduction can be attributed to the hydrophilic character of PAA-*co*-AAm. In a hydrophilic medium, the acids remain trapped within the LBL matrix rather than evaporating, thus providing continuous protonation of the PANi backbone.

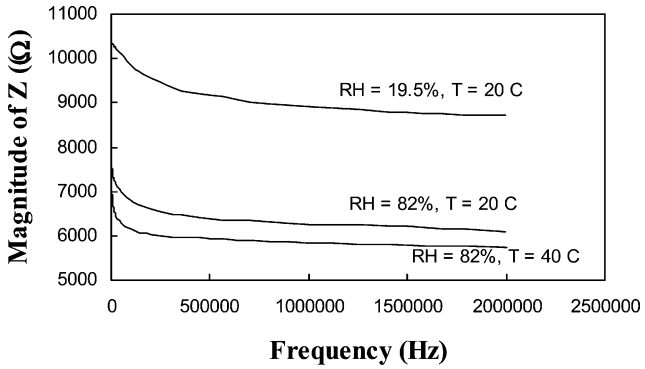


**Figure 8.** ac impedance showing that the magnitude of impedance $|Z|$ decreased from an average of 9.5 to 6.8 kΩ as a result of a change in RH from 19.5% to 82%. Increasing the temperature from 20 to 40 °C decreased $|Z|$ by ~2.3 kΩ.

**Table 2.**

| electrochemical cell purged with hydrogen gas | working electrode | electrode potential (V) |
|---|---|---|
| Pt/$H_2$/20 mM $H_2SO_4$, SCE | pure platinum | −0.329 |
| Au/$H_2$/20 mM $H_2SO_4$, SCE | pure gold | −0.022 |
| PANi/Au/$H_2$/20 mM $H_2SO_4$, SCE[a] | PANi on gold[a] | −0.006 |
| Pt−PANi/Au/$H_2$/20 mM $H_2SO_4$, SCE[b] | [b]Pt−PANi on gold[b] | −0.326 |

[a] PANi/PAA-*co*-AAm LBL film assembled on a MVD gold electrode. [b] PANi/PAA-*co*-AAm LBL film dosed with Pt clusters and assembled on an MVD gold electrode.

*Electrode Potential.* The voltage generated by a PANi/PAA-*co*-AAm LBL electrode was checked using a hydrogen-purged electrochemical cell acting as a quasireference hydrogen electrode (*q*RHE). Two background electrode potentials were obtained by measuring the open-circuit potentials (OCP ≡ voltage measured when $I \approx 0.0$ A) of platinum and gold working electrodes against a saturated calomel electrode (SCE). The SCE has a standard electrode potential equal to +0.24 V vs RHE. Therefore, our measurements should read negative against an SCE. Pure platinum was used as a background to check whether the LBL film of PANi/PAA-*co*-AAm contained any Pt clusters. On the other hand, pure gold was used as a background because the PANi/PAA-*co*-AAm LBL film was assembled on a gold film deposited by metal vapor deposition on a Nucleopore membrane, (Figure 4 Supporting Information). The results presented in Table 2 clearly show that the electrode potential of a gold-coated LBL film of PANi/PAA-*co*-AAm (i.e., Au/PANi/PAA-*co*-AAm LBL electrode) that was not loaded with platinum and acting as a *q*RHE is equal to −0.006 V, indicating a behavior similar to that of a pure gold electrode

of OCP = −0.022 V. A voltage difference of only 0.016 V implies a very small contribution to potential from the LBL film. However, when the same LBL electrode was dosed with Pt black by being soaked in $PtCl_6^{2-}$ salt solution and then reduced with $NaBH_4$, it yielded an electrode potential of −0.326 V, showing that the Pt clusters are electronically communicating within the conducting PANi backbone. An electrode potential value of −0.326 V rather than −0.24 V is expected because the activity of $H^+$ is not standard (i.e., $a_{H+} \neq 1.0$), but $a_{H+} \approx 0.04$ in the solution under study.

At this juncture, efforts are underway to assemble a complete "soft" membrane−electrode assembly (MEA) using LBL PANi electrodes and LBL composite membranes for power generation. Apart from the catalyst, a polyaniline-based LBL MEA is very different from conventional MEAs in terms of materials and structure. This difference would have a major impact in reducing the cost of MEAs as well as making them robust for microfuel-cell fabrication.

## Conclusion

Polyaniline (PANi) conducting polymer was used with polyanions of PAA, PAA-*co*-PAAm, and PAMPS to assemble LBL thin film electrodes. The PANi LBL electrodes exhibited a continuous, nonporous structure when assembled with the PANi solution at pH 2.5 and the polyanionic solution at pH 4.0. A porous LBL film was obtained when PANi at pH 2.5 was assembled with PAA or PAA-*co*-PAAm at pH 6.0; the porous matrix was advantageous and led to higher ionic conductivity. Three methods were used to incorporate catalytic amounts of platinum into the LBL thin films. The platinum was layered directly into the multilayer composite using electrostatically stabilized platinum particles; the platinum was complexed with PANi in solution prior to assembly and then incorporated into the multilayer; and finally, the PANi/polyanion multilayers were first assembled and then loaded with platinum by reductive precipitation of platinum salt, $PtCl_6^{2-}$, inside the LBL film. Of the three approaches to catalyst loading and the two PANi/polyanion electrodes studied, the PANi/PAA-*co*-PAAm electrode loaded through reductive precipitation of platinum salts exhibited the most optimal film morphology, so its electrochemical properties were then studied. An ionic conductivity of $3.6 \times 10^{-5}$ S cm$^{-1}$ was measured when a PANi/PAA-*co*-PAAm film was dosed with NaCl at pH 8; thus, higher conduction is expected when the film is doped with acids, as would be the case during operation. The PANi/PAA-*co*-PAAm electrodes exhibited a relatively high electronic conductivity of 1.0−2.3 S cm$^{-1}$ and were remarkably stable under ambient conditions. Voltage signals under potentiostatic control did not degrade in hours. Three different methods were used to test platinum loading. The most effective was the reductive precipitation of platinum salt inside the LBL film using sodium borohydride to achieve an acceptable platinum content of 0.3 mg cm$^{-2}$. Using a hydrogen-purged galvanic cell against a saturated calomel electrode, an electrode potential of −0.326 V was recorded, which is close to the electrode potential of pure platinum.

**Acknowledgment.** The authors thank the Center of Material Science and Engineering at Massachusetts Institute of Technology and the Chemical Transport Systems Program of the Engineering Division of the National Science Foundation for the financial support of this project (Grant CTS-0136029). Additional support was provided by the Office of Naval Research Polymers Program.

**Supporting Information Available:** Four additional figures. This material is available free of charge via the Internet at http://pubs.acs.org.

CM051335O